Supplemental Figures

Fig. S1. Sequence and topology of *N.gonorrhoeae* MtrF. Related to Figure 1. Alignment of the amino acid sequences of the AbgT family of transporters was done using CLUSTAL W. *, identical residues; :, >60% homologous residues. Secondary structural elements are indicated: TM, transmembrane helix; α, helix. The sequence and topology of *N. gonorrhoeae* MtrF are shown at the top. Conserved residues involved in lining the channel of the inner core of the protein are highlight with green bars.

Fig. S2. Stereo view of the electron density maps of MtrF at a resolution of 3.95 Å. Related to Figure 1. (a) The electron density maps are contoured at 1.2 σ. The Cα traces of the MtrF dimer in the asymmetric unit are included. Anomalous signals of the four $Ta_6Br_{12}^{2+}$ and six $W_6(\mu\text{-}O)_6(\mu\text{-}Cl)_6Cl_6^{2-}$ cluster sites (both contoured at 4 σ) found in the asymmetric unit are colored red and white, respectively. (b) Anomalous maps of the 30 selenium sites (contoured at 4 σ). Two protomers forming a dimer of MtrF are found in the asymmetric unit. Each protomer contributes 15 selenium sites corresponding to the 15 methionines (red). The Cα traces of the two MtrF monomers are colored green and cyan. (c) Representative section of the electron density at the interface of TM2 and TM6 of MtrF. The electron density (colored slate) is contoured at the 1.2 σ level and superimposed with the final refined model (green, carbon; red, oxygen; blue, nitrogen).

Fig. S3. Representative gel filtration experiment. Related to Figure 1. The experiment demonstrated that MtrF exists as a dimer in solution. The *y* axis values were defined as: $K_{av} = (V_e - V_0)/(V_T - V_0)$, where V_T, V_e, and V_0 are the total column volume, elution

volume, and void volume of the column, respectively. Standards used were the trimeric *E. coli* CusC channel (M_r 12,400) and monomeric *N. gonorrhoeae* NorM efflux pump (M_r 29,000). The void volume was measured using blue dextran (M_r 2,000,000).

Fig. S4. Surface representation of a cross section of the MtrF protomer. Related to Figure 2. The channel formed within the outer core of the MtrF protomer is colored purple.

Fig. S5. Expression level of the MtrF pumps. Related to Figure 3. An immunoblot against MtrF of crude extracts from 50 μg dry cells of strain BL21(DE3)Δ*abgT*Δ*pabA* expressing the MtrF wild-type and mutant (D193A, S417A, W420A, P438A, R446A, D449A, and P457A) pumps are shown.

Fig. S6. Copy numbers of MtrF in the cell. Related to Figure 3. An immunoblot against MtrF of crude extracts from 1.1 x 10^9 cells of BL21(DE3)Δ*abgT*Δ*pabA*/pET15bΩ*mtrF* (lane 1). 6 ng (lane 2), 12 ng (lane 3), 30 ng (lane 4), 60 ng (lane 5), 120 ng (lane 6) and 300 ng (lane 7) of the purified MtrF protein were used as standards. The program ImageJ (Schneider et al., 2012) suggests that the crude cell extracts contain 21 ng MtrF protein, which should correspond to ~200 copies per cell.

Fig. S7. Representative isothermal titration calorimetry for the binding of sulfanilamide to MtrF. Related to Figure 5. (a) Each peak corresponds to the injection of 10 μl of 40 μM monomeric MtrF in buffer containing 20 mM Tris-HCl pH 7.5 and 0.03% DDM into

the reaction containing 1.0 mM sulfanilamide in the same buffer. (b) Cumulative heat of reaction is displayed as a function of the injection number. The solid line is the least-square fit to the experimental data, giving a K_D of 1.14 ± 0.01 μM.

Supplemental References

Schneider, C.A., Rasband, W.S., and Eliceiri, K.W. (2012). NIH Image to ImageJ: 25 years of image analysis. Nature Methods *9*, 671-675.

Figure S1

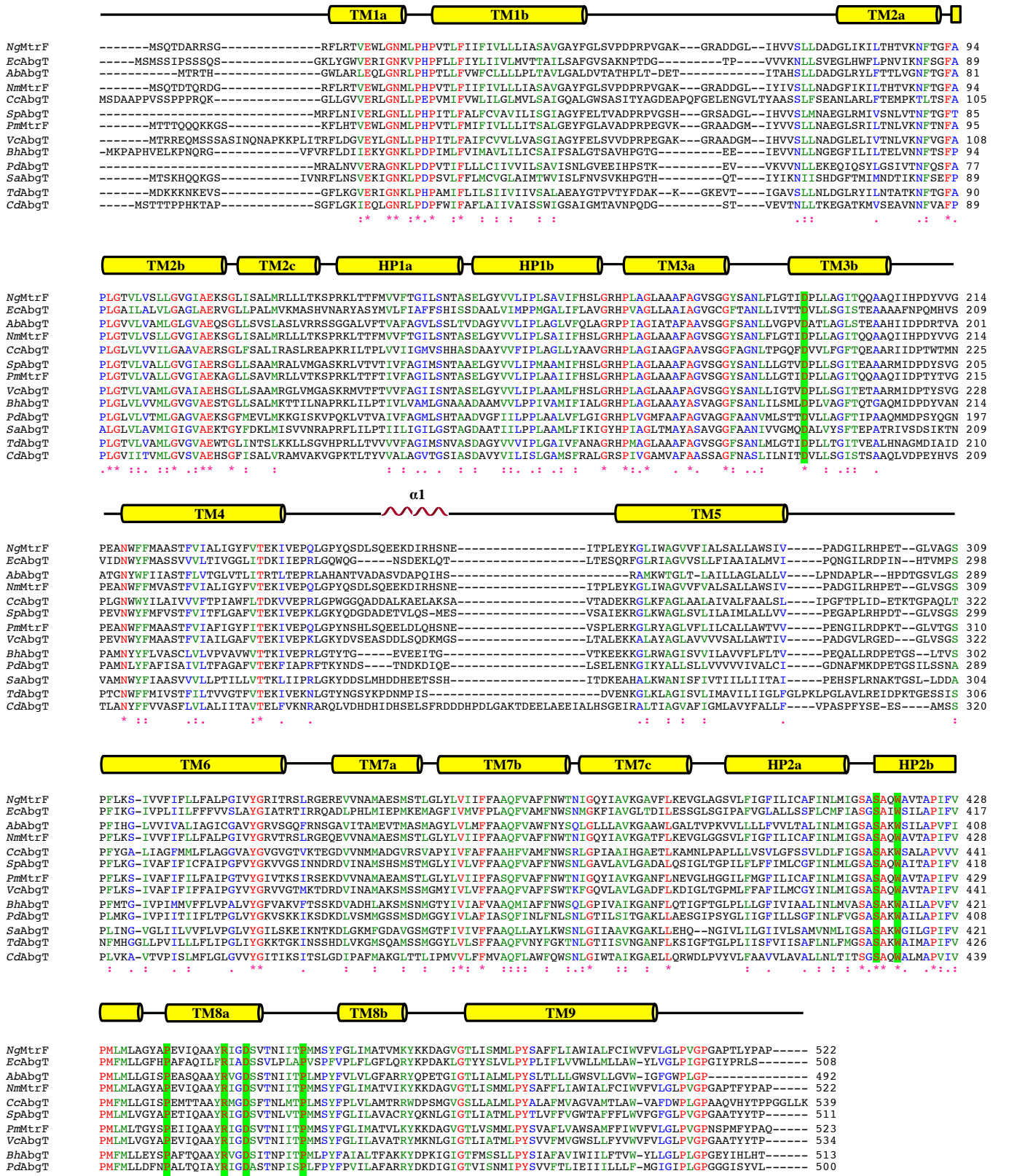
TM1a
TM1b
TM2a
TM2b
TM2c
HP1a
HP1b
TM3a
TM3b
α1
TM4
TM5
TM6
TM7a
TM7b
TM7c
HP2a
HP2b
TM8a
TM8b
TM9
NgMtrF
EcAbgT
AbAbgT
NmMtrF
CcAbgT
SpAbgT
PmMtrF
VcAbgT
BhAbgT
PdAbgT
SaAbgT
TdAbgT
CdAbgT

Figure S2

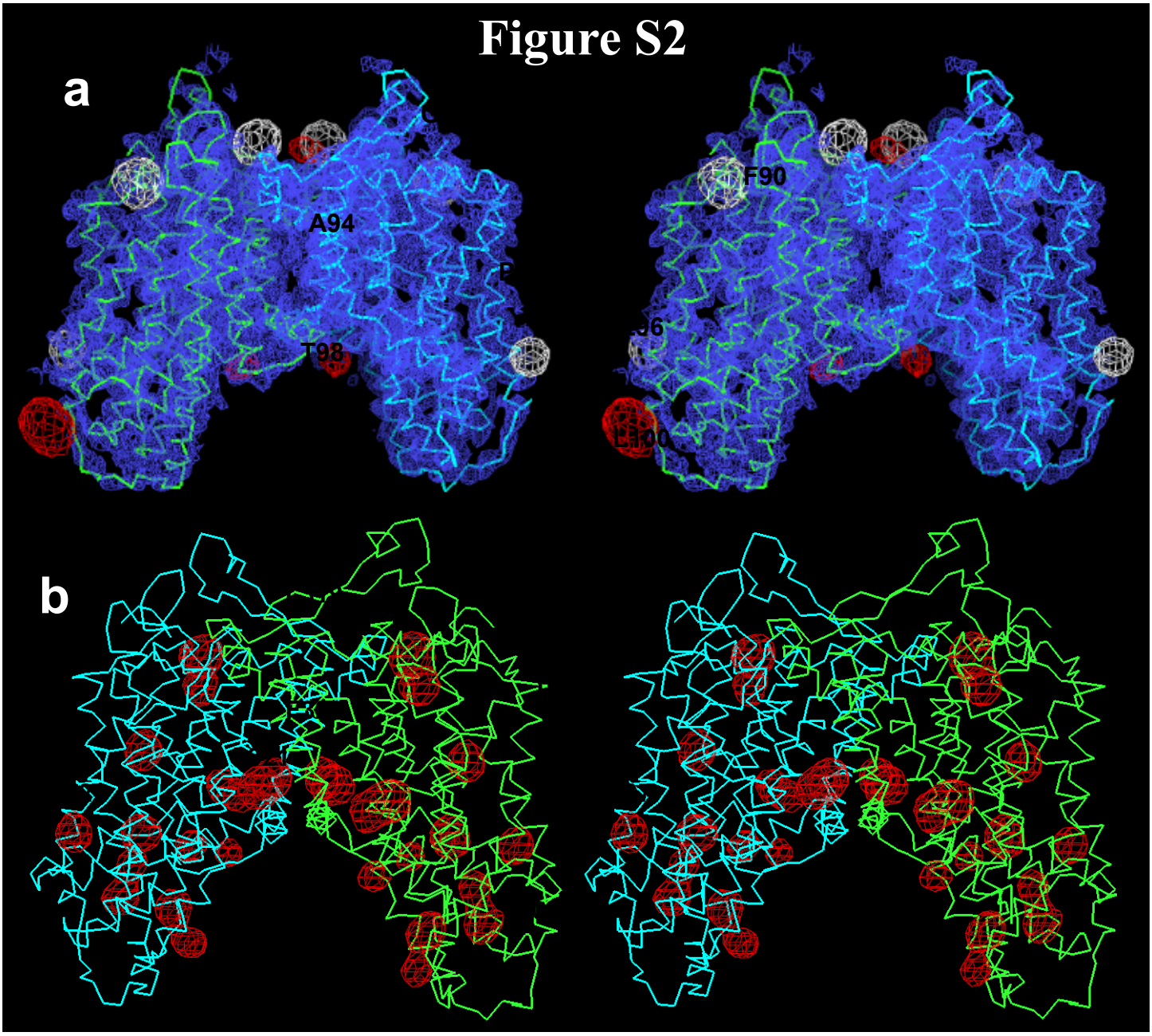
a
A94
T98
F90
b

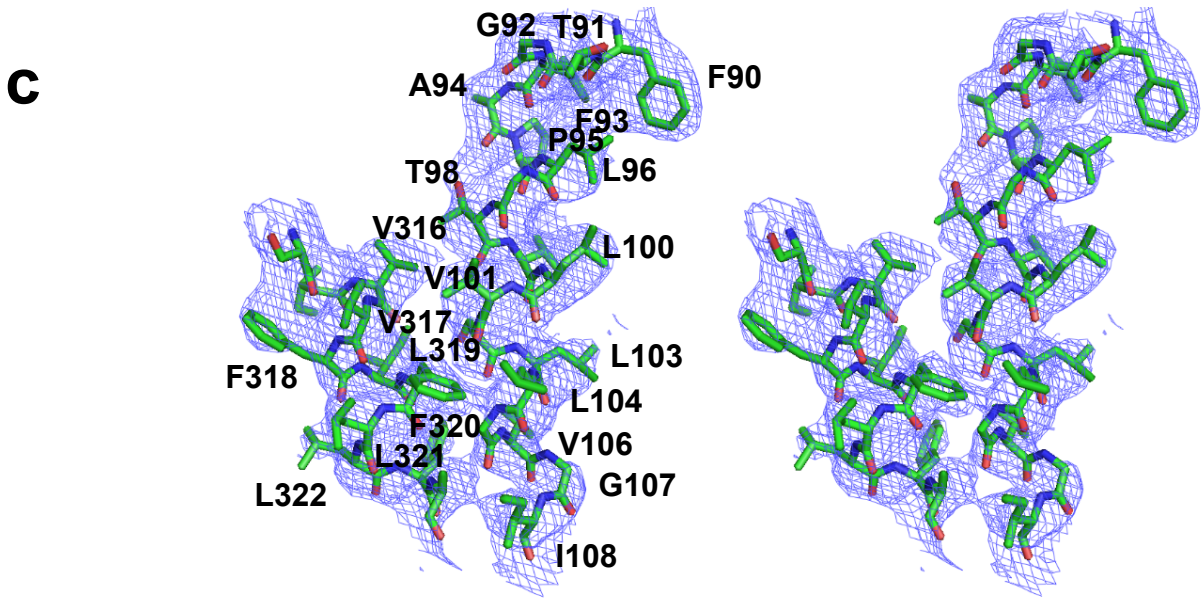
c
G92
T91
A94
F90
F93
P95
T98
L96
V316
L100
V101
V317
L319
L103
F318
L104
F320
V106
L321
G107
L322
I108

Figure S3

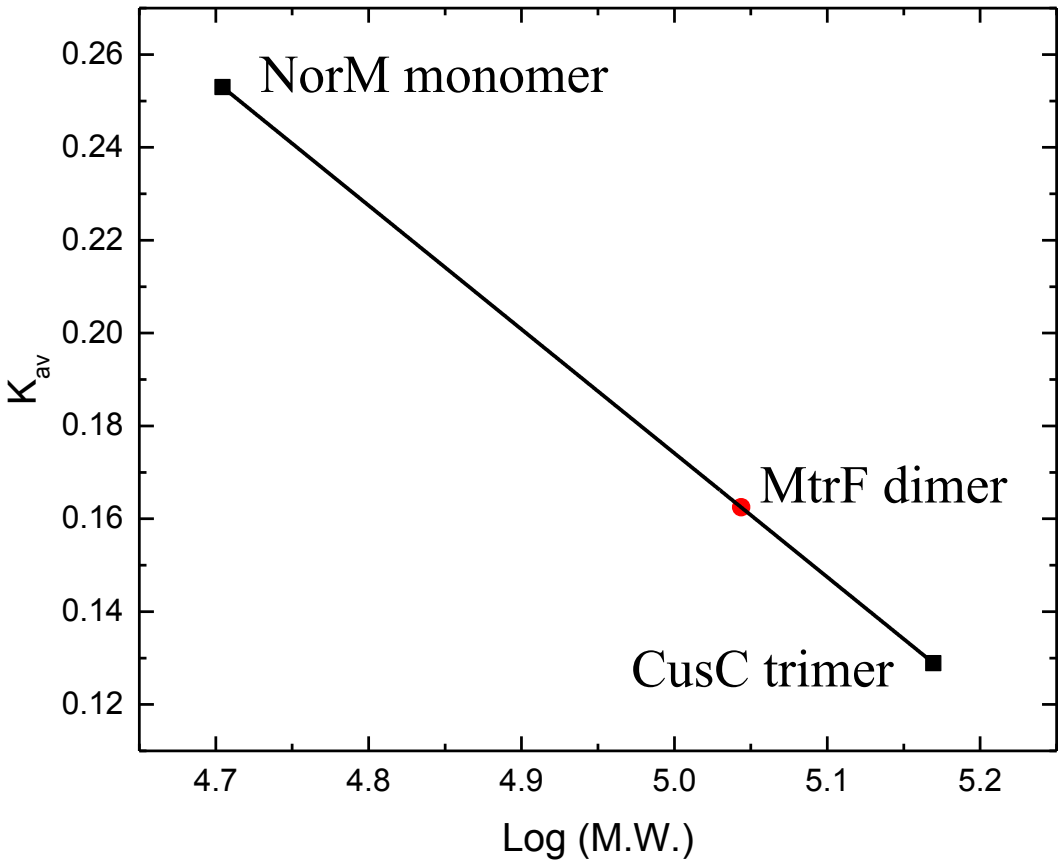
NorM monomer
MtrF dimer
CusC trimer
0.26
0.24
0.22
0.20
0.18
0.16
0.14
0.12
K_{av}
4.7
4.8
4.9
5.0
5.1
5.2
Log (M.W.)

Figure S4

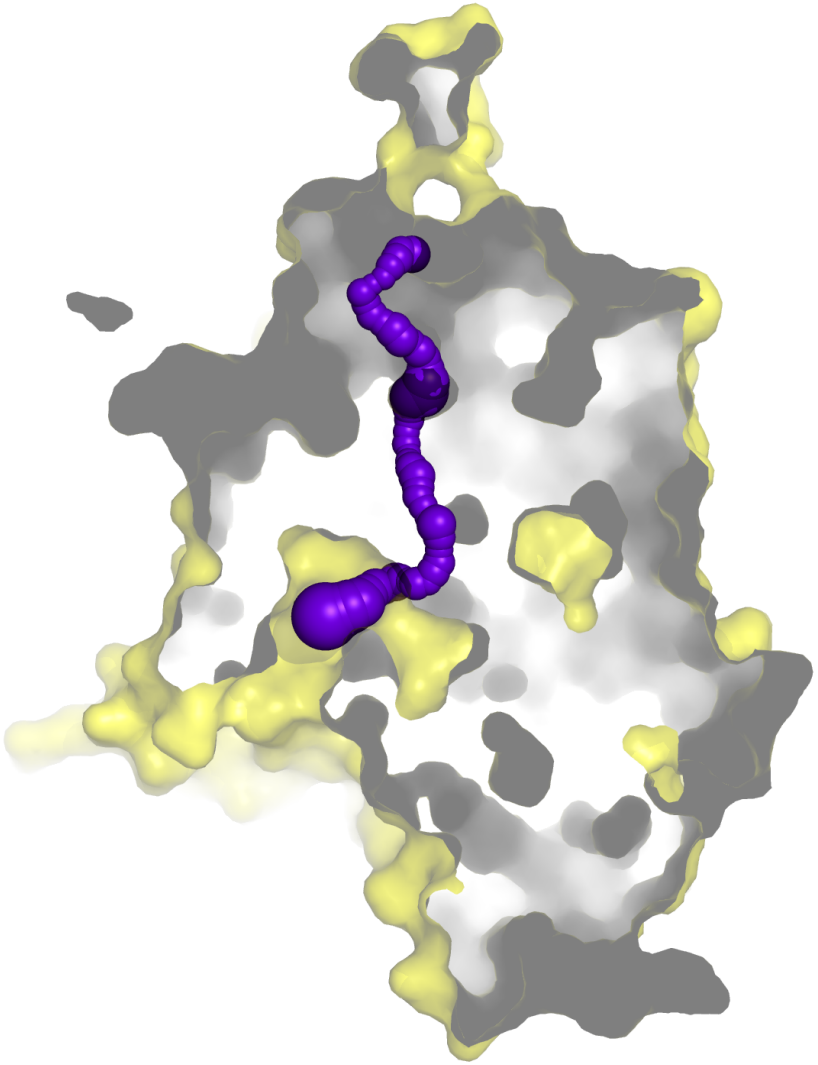

Figure S5

Figure S6

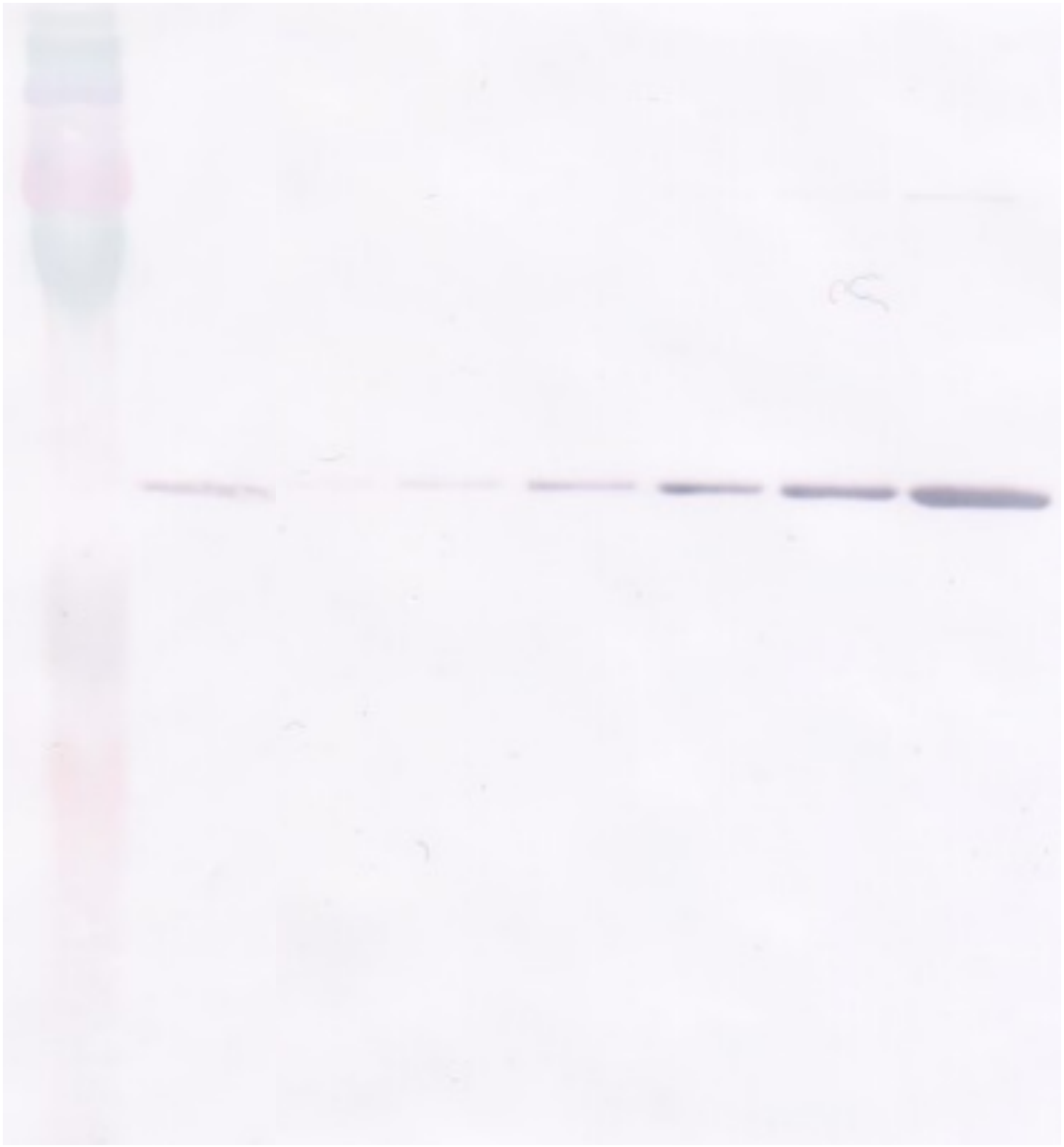

1 2 3 4 5 6 7

Figure S7

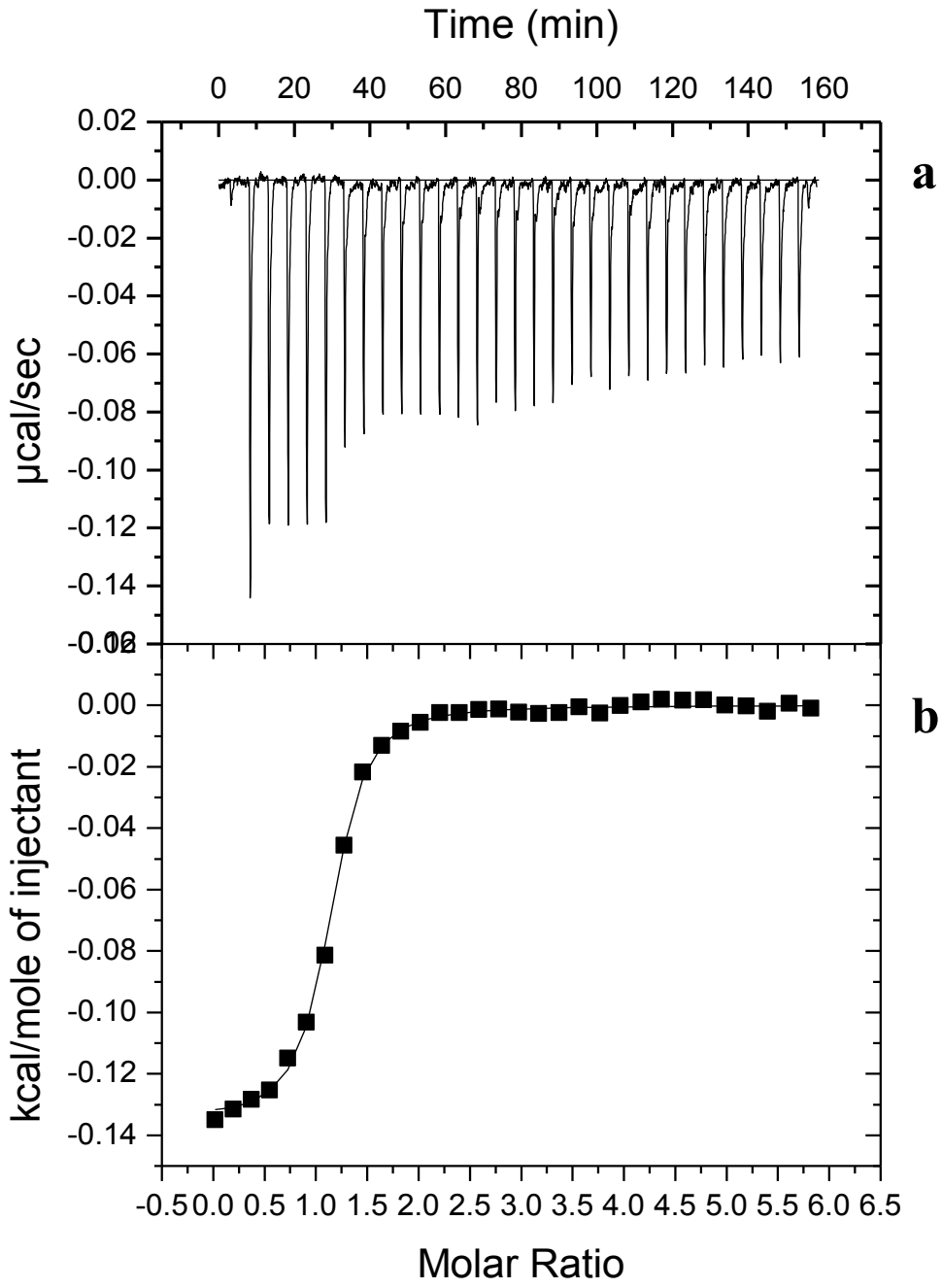
Time (min)
0 20 40 60 80 100 120 140 160
0.02
0.00
-0.02
-0.04
-0.06
-0.08
-0.10
-0.12
-0.14
µcal/sec
a
0.00
-0.02
-0.04
-0.06
-0.08
-0.10
-0.12
-0.14
kcal/mole of injectant
b
-0.5 0.0 0.5 1.0 1.5 2.0 2.5 3.0 3.5 4.0 4.5 5.0 5.5 6.0 6.5
Molar Ratio

Table S1. Data collection, phasing and structural refinement statistics. Related to Figure 1.

Data set	Native MtrF	$Ta_6Br_{12}^{2+}$	$W_6(\mu\text{-}O)_6(\mu\text{-}Cl)_6Cl_6^{2-}$	Se (peak)
Data Collection				
Wavelength (Å)	0.98	1.25	1.02	0.98
Space group	$P6_5$	$P6_5$	$P6_5$	$P6_5$
Resolution (Å)	50 – 3.95 (4.11 – 3.95)	50 – 6.53 (6.74 – 6.53)	50 – 5.70 (5.93 – 5.70)	50 – 4.60 (4.76 – 4.60)
Cell constants (Å)				
a	120.77	120.57	120.51	116.37
b	120.77	120.57	120.51	116.37
c	233.90	231.33	231.75	224.88
α, β, γ (°)	90, 90, 120	90, 90, 120	90, 90, 120	90, 90, 120
Molecules in ASU	2	2	2	2
Redundancy	4.7 (4.0)	5.7 (5.8)	5.6 (6.5)	4.4 (3.8)
Total reflections	868,348	28,1275	189,1056	1796,647
Unique reflections	16,832	3814	5533	9712
Completeness (%)	98.2 (92.8)	99.9 (99.9)	99.7 (99.0)	99.9 (100)
R_{merge} (%)	5.8 (46.8)	5.3 (49.5)	8.6 (48.7)	9.4 (59.0)
I / σ	29.65 (0.88)	45.42 (2.60)	34.14 (1.7)	19.35 (1.95)
Phasing				
Number of sites		4	6	30
Phasing power (acentric/centric)		1.71/0.99		
Figure of merit		0.59		
Refinement	MtrF			
Resolution (Å)	50 – 3.95			
R_{work} (%)	29.9			
R_{free} (%)	33.6			
RMSD bond lengths (Å)	0.009			
RMSD bond angles (°)	1.52			
Ramachandran plot				
most favoured (%)	89.0			
additional allowed (%)	10.0			
generously allowed (%)	1.0			
disallowed (%)	0.0			

Table S2. Primers for site-directed mutagenesis. Related to Figure 3.

Primer	Sequence
D193A-forward	5′-CTGTTCCTGGGCACCATTGCTCCGCTGCTGGCCGGTATC-3′
D193A-reverse	5′-GATACCGGCCAGCAGCGGAGCAATGGTGCCCAGGAACAG-3′
S417A-forward	5′-GGTAGTGCTGCCGCACAATGGGCAGTGACCGCACCGATCT-3′
S417A-reverse	5′-CCATTGTGCGGCAGCACTACCGATCATCAGGTTAATAAA-3′
W420A-forward	5′-CGCACAAGCGGCAGTGACCGCACCGATCTTCGTTCCG-3′
W420A-reverse	5′-GGTCACTGCCGCTTGTGCGGAAGCACTACCGATCATCAG-3′
P438A-forward	5′-GGCTATGCTGCGGAAGTCATTCAGGCCGCATACCGC-3′
P438A-reverse	5′-GACTTCCGCAGCATAGCCTGCCAGCATCAGCATCGG-3′
R446A-forward	5′-GTCATTCAGGCCGCATACGCCATCGGTGATTCAGTTACC-3′
R446A-reverse	5′-GGTAACTGAATCACCGATGGCGTATGCGGCCTGAATGAC-3′
D449A-forward	5′-GCCGCATACCGCATCGGTGCTTCAGTTACCAATATTATC-3′
D449A-reverse	5′-GATAATATTGGTAACTGAAGCACCGATGCGGTATGCGGC-3′
P457A-forward	5′-ATCACGGCGATGATGTCGTATTTTGGTCTGATTATG-3′
P457A-reverse	5′-CGACATCATCGCCGTGATAATATTGGTAACTGAATC-3′

Table S3. MICs of sulfamethazine, sulfadiazine, sulfathiazole and sulfanilamide for different MtrF variants expressed in *E. coli* BL21(DE3)Δ*abgT*Δ*pabA*. Related to Figure 5.

Gene in BL21(DE3)Δ*abgT*Δ*pabA*	Sulfamethazine (μg/mL)	Sulfadiazine (μg/mL)	Sulfathiazole (μg/mL)	Sulfanilamide (μg/mL)
Empty vector	62.5	31.25	62.5	500
mtrF (wild-type)	2000	>250	>500	4000
mtrF (D193A)	1000	31.25	62.5	2000
mtrF (S417A)	125	31.25	125	2000
mtrF (W420A)	125	31.25	62.5	2000
mtrF (P438A)	62.5	31.25	62.5	1000
mtrF (R446A)	1000	>250	>500	2000
mtrF (D449A)	62.5	31.25	62.5	1000
mtrF (P457A)	62.5	62.5	125	1000

Table S4. Binding of sulfamethazine, sulfadiazine, sulfathiazole, sulfanilamide and *p*-aminobenzoic acid by MtrF. Related to Figure 5.

	K_D (μM)	ΔH (kcal•mol^{-1})	ΔS (cal•mol•deg^{-1})
Sulfamethazine	0.33 ± 0.02	-580.2 ± 5.9	27.7
Sulfadiazine	12.74 ± 0.62	-1900.0 ± 131.8	16.0
Sulfathiazole	1.52 ± 0.07	-267.3 ± 8.0	25.7
Sulfanilamide	1.14 ± 0.01	-135.2 ± 1.1	26.7
PABA	0.54 ± 0.02	-319.2 ± 8.6	27.6

Table S5. Binding of sulfamethazine, sulfadiazine, sulfathiazole, sulfanilamide and *p*-aminobenzoic acid by the W420A mutant. Related to Figure 5.

	K_D (μM)	ΔH (kcal•mol^{-1})	ΔS (cal•mol•deg^{-1})
Sulfamethazine	10.78 ± 1.17	-233.4 ± 10.7	21.9
Sulfadiazine	105.82 ± 25.6	-41103 ± 2065.0	4.4
Sulfathiazole	50.76 ± 8.9	-713.5 ± 28.4	17.3
Sulfanilamide	6.80 ± 1.5	-63.1 ± 3.0	23.4
PABA	41.15 ± 8.5	-425.3 ± 18.7	18.6